Research Journal of Recent Sciences _____ ISSN 2277-2502
Vol. **3(4),** 63-70, April **(2014)** *Res.J.Recent Sci.*

Analysis of Shear-thinning Fluid motion in Taylor–Couette flow

Masoumifard Mohammad[1*], Norouzi, Rouhollah[1], Nezamkhiavy Khosro[2]
[1*]Department of Mechanical Engineering, Meshkinshahr Branch, Islamic Azad University, Meshkinshahr, IRAN
[2]Young Researchers and Elite Club, Meshkinshahr Branch, Islamic Azad University, Meshkinshahr, IRAN

Available online at: www.isca.in, www.isca.me
Received 7th December 2013, revised 3rd February 2014, accepted 1st March 2014

Abstract

Viscosity of the shear-thinning fluid depends on the shear rate. This study is conducted in Taylor vortex flow conditioned by the rotation of inner cylinder and stillness of outer cylinder and just taking into account the axial flow for estimating the parameters of flow (velocity and pressure components) in the narrow gap between two cylinders. The results of this study are important in the bearing application. The equations of Taylor–Couette flow and Galerkin method were obtained by the equations for the conservation of mass and momentum equations. Flow parameters were obtained by Fortran and investigated by Mathematica software. The flow is the sum of base flow and a deviation from the base flow. According to the main results of analysis above, the target diagrams are compared with Newtonian and a_1 diagrams. The more the value of parameter a_2 is reduced, the quicker the flow will become critical. All components of real velocity and pressure are reduced while increasing Shear-thinning.

Keywords: Shear-thinning, viscosity, shear rate, Taylor–Couette flow.

Introduction

Taylor indicated that if the relative velocity between two cylinders exceeds a certain limit, the form of flow will be changed into the horizontal vortices, in situ (independent of time) and symmetric to the cylinder axis, called "Taylor vortex flow" (TVF). The cylindrical longitudinal oscillation period will be $2\pi/2k = \pi/k$[1].

Kuhlmann examined the TVF in a narrow gap when the inner cylinder was rotating at angular velocity fluctuations in a period of time[2] and simplified Navier-Stokes equations with the finite difference method according to Galerkin. The thermal displacement formulas in viscoelastic and shear-thinning fluids have recently been investigated[1].

The dependence of the parameters together creates the limitations in this analysis; some of the available parameters such as μ_0, n, λ are experimental. Zeidler et al's diagram, which is obtained from simulating the following table, is one of the best experimental sources for selecting the values[1].

According to the general hypotheses, the fluid is considered incompressible, the cylinders rigid and long and the radius of inner cylinder (R_1) is equal to 50 cm and the gap ratio (d) equal to 2mm; the outer cylinder is stationary and the inner cylinder has the angular velocity (Ω) which is the integer multiple of π. Here, the value of 2π is considered and due to the axial symmetry in this analysis, $\frac{\partial}{\partial\theta}$ is considered equal to zero and also the density is 1000 Kg / m^3.

Considered Equations

The equations for the conservation of mass and momentum[3] in cylindrical coordinates are as follows:

$$\nabla U = 0 \quad (1)$$

$$\rho(U_{,T} + U.\nabla U) = -\nabla P + \nabla.(\mu\Gamma) \quad (2)$$

In the above equations,

$$U = (U_R, U_\theta, U_Z)^T \quad , \quad \Gamma = \nabla U + (\nabla U)^T$$

Table-1

Considered values for $\alpha_1, \alpha_2, \mu_0$ [4]

	$\alpha_1 = -0.075$ $\alpha_2 = -0.002$	$\alpha_1 = -0.05$ $\alpha_2 = -0.002$	$\alpha_1 = -0.025$ $\alpha_2 = -0.002$	$\alpha_1 = -0.01,$ $\alpha_2 = -0.002$	$\alpha_1 = 0.0,$ $\alpha_2 = 0.00$
μ_0 (pa.s)	0.0044	0.0043	0.0042	0.0041	0.004

Given the multiplicity of available variables, the dimensionless parameters with the first-order values and coefficients in the equations should be applied[4]. The dimensionless parameters with such this condition are as follows:

$$x=\frac{r-R_1}{d},\ z=\frac{Z}{d},\ t=\frac{\upsilon_0}{d^2}T,\ p=\frac{d^2}{\rho\upsilon_0^2}P \qquad (3)$$

$$u_x=\frac{d}{\upsilon_0}V_r,\ u_y=\frac{1}{R_1\Omega}V_\theta,\ u_z=\frac{d}{\upsilon_0}V_z,\ \eta=\frac{\mu}{\mu_0}$$

The dimensionless and real parameters are shown with large and small indices respectively. According to the equations (1), (2) and (3) and the boundary conditions governing the laminar flow, we have:

$$V_\theta^0(r=R_1)=R_1\Omega \quad , \quad V_\theta^0(r=R_2)=0 \quad , \quad u_x^0=u_z^0=0$$

$$\Rightarrow V_\theta^0=\frac{R_1\Omega(R_2-r)}{d} \Rightarrow u_y^0=1-x \qquad (4)$$

$$p_{,x}^0=Ta(u_y^0)^2=Ta(1-x)^2$$

In general, the rotational speed of cylinders relative to each other is not the only determining factor for the beginning of vortex flow, but the other factors such as the size of the gap, radius of flow, and the viscosity of fluid are effective in this regard and the changes in only one of them can change the time of creating the vortices or their types. Therefore, the following dimensionless numbers are defined[1]:

$$Re=\frac{\Omega R_1 d}{\upsilon_0} \qquad \varepsilon=\frac{d}{R_1} \qquad Ta=Re^2\varepsilon \qquad (5)$$

Where, Re is Reynolds number, ε: The ratio of gap size to the radius, and Ta: Taylor number. Furthermore, Ω: Relative angular velocity of two cylinders (in this case the angular velocity of inner cylinder), R_1: The radius of inner cylinder, d: Size of gap and υ_0: Kinematics viscosity at zero shear rate.[1]

The presented mathematical model is called Carreau-Yasuda model as follows:

$$\frac{\eta-\eta_\infty}{\eta_0-\eta_\infty}=\left[1+(\lambda\dot\gamma)^a\right]^{\frac{n-1}{a}} \qquad (6)$$

This equation depends on five experimental parameters including η_0 ،η_∞ ،λ ،n , and a. In equation (6) η is the apparent shear viscosity (dynamic) and $\dot\gamma$ is the same as the D or the shear rate; and a is the dimensionless quantity which represents the effect of transition from the stable region η to the exponential region. According to the performed experiments, a = 2 and η_∞ converges to zero and λ is a time inverse constant of shear rate per which the shear-thinning behavior begins.[1]

The dependence of viscosity on the shear rate can be found according to the equations (6) and (3) in which μ is the real viscosity, η the dimensionless viscosity, $\dot\Gamma$ the real shear rate and $\dot\gamma$ the dimensionless shear rate. The following equation is defined between $\dot\Gamma$ and $\dot\gamma$: [1]

$$\dot\gamma=\frac{d}{R_1\Omega}\dot\Gamma \qquad (7)$$

The equation (6) will be as follows in terms of $\dot\gamma$ through introducing the dimensionless number $De=\frac{\lambda R_1\Omega}{d}$ and naming $S=\frac{\mu_\infty}{\mu_0}$; :[1]

$$\eta(\dot\gamma)=S+(1-S)\left[1+(De\,\dot\gamma)^2\right]^{\left(\frac{n-1}{2}\right)} \qquad (8)$$

Since our fluid is shear-thinning ($1<\frac{n-1}{2}<0$), thus the equation (8) is simplified as follows by extending three terms of above equation and defining $\alpha_1=(1-S)\left(\frac{n-1}{2}\right)De^2$ and

$$\alpha_2=(1-S)\left[\left(\frac{(n-1)(n-3)}{4}\right)(De)^4\right]:$$

$$\eta(\dot\gamma)=1+\alpha_1\dot\gamma^2+\alpha_2\dot\gamma^4 \qquad (9)$$

α_1,α_2 are the important coefficients which cover the rheological properties ($\dot\gamma,n,S$), geometrical properties and boundary conditions (d,Ω,R_1). The relationship among α_1,α_2,De indicates that the amounts of α_1,α_2 should also be small. α_1,α_2 is positive for shear-thickening fluids, negative for shear-thinning fluids and zero for Newtonian fluids. Thus, the amounts of α_1,α_2 will be negative for our fluid. Now, if $\alpha_2=0$, our fluid will become weakly-shear-thinning.

Given that $u_{y,x}^0=-1$ and $u_{y,z}^0=0$, for the laminar flow we have:

$$\eta^0=1+\alpha_1+\alpha_2 \qquad (10)$$

In the overall state, it is better to write the conservation and viscosity equations in terms of total terms of laminar flow and diversion towards it in order to obtain the better control over

both flow; it is worth noting that there is only v_θ in the laminar flow, but all three viscosities existed in the deviation flow.

For simplicity and through inserting the values obtained from the analysis of laminar flow in the equations (1) and (2), we consider $\eta' = \eta, u_x' = u$, $u_y' = \upsilon$, $u_z' = w$ and $P' = P$, thus:

$$u_{,x} + w_{,z} = 0$$

$$u_{,t} + uu_{,x} + wu_{,z} - Ta\upsilon^2 - 2Ta\upsilon(1-x) =$$
$$-P_{,x} + (\eta^0 + \eta)(u_{,xx} + u_{,zz}) + 2\eta_{,x}u_{,x} + \eta_{,z}(u_{,z} + w_{,x})$$
$$\upsilon_{,t} + u\upsilon_{,x} + w\upsilon_{,z} =$$
$$u + (\eta^0 + \eta)(\upsilon_{,xx} + \upsilon_{,zz}) + \eta_{,z}\upsilon_{,z} + \eta_{,x}(\upsilon_{,x} - 1)$$
$$w_{,t} + uw_{,x} + ww_{,z} = \quad (11)$$
$$-P_{,z} + (\eta^0 + \eta)(w_{,xx} + w_{,zz}) + 2\eta_{,z}w_{,z} + \eta_{,x}(u_{,z} + w_{,x})$$

Galerkin Image Method is considered for solving the equations and the dominant modes are as follows according to the performed experiments: [5]

$$u_x(x,z,t) = u_{11}(t)\sin\pi x\cos kz$$
$$u_y(x,z,t) = \upsilon_{10}(t)\sin\pi x + \upsilon_{11}(t)\sin\pi x\cos kz + \upsilon_{20}(t)\sin 2\pi x$$
$$u_z(x,z,t) = w_{11}(t)\cos\pi x\sin kz$$
$$p(x,z,t) = p_{11}(t)\cos\pi x\cos kz \quad (12)$$

The components, $\upsilon_{10}(t)$, $\upsilon_{11}(t)$, $\upsilon_{20}(t)$, $w_{11}(t)$, $p_{11}(t)$ and $u_{11}(t)$ are dimensionless. In order to make the obtained values for three components of velocity close to each other and within the interval [0,1], the following scaled velocities are defined as follows: [6]

$$u = \frac{\pi\tau}{\sqrt{2}}u_{11}(t) \quad , \quad \upsilon = \frac{\pi}{\sqrt{2}}\upsilon_{11}(t) \quad , \quad w = -\pi\upsilon_{20}(t) \quad (13)$$

We insert the equations (12) in the equations (11) and integrate the equations for the conservation of mass and equations (13) at the interval $z \in \left[0, \pi/k\right]$ and $x \in [0,1]$ in a period. This is done in two steps, and the scaled velocities become as follows by defining the important quantity, reduced Taylor number, as $r = Ta\tau^3k^2$:

$$\dot{u} = r\upsilon - u$$
$$+\alpha_1(-u + A_1u\upsilon^2 + A_2uw + A_3uw^2) + \alpha_2(-u + A_4u\upsilon^2 + A_5u\upsilon^4$$
$$+A_6uw + A_7u\upsilon^2w + A_8uw^2 + A_9u\upsilon^2w^2 + A_{10}uw^3 + A_{11}uw^4$$
$$\dot{\upsilon} = -uw + u - \upsilon + \alpha_1(B_1\upsilon + B_2\upsilon^3 + B_3\upsilon w + B_4\upsilon W^2)$$
$$+\alpha_2(B_5\upsilon + B_6\upsilon^3 + B_7\upsilon^5 + B_8\upsilon w + B_9\upsilon^3w + B_{10}\upsilon w^2 + B_{11}\upsilon^3w^2 \quad (14)$$
$$+B_{12}\upsilon w^3 + B_{13}\upsilon w^4)$$
$$\dot{w} = u\upsilon - C_1w + \alpha_1(C_2\upsilon^2 + C_3w + C_4\upsilon^2w + C_5w^3)$$
$$+\alpha_2(C_6\upsilon^2 + C_7\upsilon^4 + C_8w + C_9\upsilon^2w + C_{10}\upsilon^4w + C_{11}w^2 + C_{12}\upsilon^2w^2$$
$$+C_{13}w^3 + C_{14}\upsilon^2w^3 + C_{15}w^4 + C_{16}w^5)$$

The coefficients A_1 to C_{16} are : Coefficients of equations (14)

$$A_1 = -\frac{9k^6 - 13k^4\pi^2 + 43k^2\pi^4 + \pi^6}{8\pi^2(k^2+\pi^2)^2} \quad , \quad A_2 = \frac{2(k^2-\pi^2)^2}{(k^2+\pi^2)^2} \quad , \quad A_3 = \frac{2(-k^2+\pi^2)}{k^2+\pi^2} \quad ,$$

$$A_4 = -\frac{9k^6 - 11k^4\pi^2 + 111k^2\pi^4 + 3\pi^6}{8\pi^2(k^2+\pi^2)^2} \quad , \quad A_5 = -\frac{25k^8 - 44k^6\pi^2 + 34k^4\pi^4 + 56k^2\pi^6 + \pi^8}{16\pi^4(k^2+\pi^2)^2} \quad ,$$

$$A_6 = -\frac{4(k^4 - 6k^2\pi^2 + \pi^4)}{(k^2+\pi^2)^2} \quad , \quad A_7 = -\frac{6k^2(k^4 - 2k^2\pi^2 - 11\pi^4)}{\pi^2(k^2+\pi^2)^2} \quad , \quad A_8 = -12 \quad ,$$

$$A_9 = -\frac{7k^6 - 11k^4\pi^2 + 177k^2\pi^4 + 3\pi^6}{4\pi^2(k^2+\pi^2)^2} \quad , \quad A_{10} = \frac{12(k^4 - 6k^2\pi^2 + \pi^4)}{(k^2+\pi^2)^2} \quad , \quad A_{11} = -6 \quad , \quad B_1 = -\frac{k^2+3\pi^2}{k^2+\pi^2} \quad ,$$

$$B_2 = -\frac{9k^4 + 2k^2\pi^2 + 9\pi^4}{8\pi^2(k^2+\pi^2)^2} \quad , \quad B_3 = \frac{2(-k+\pi)(k+\pi)}{k^2+\pi^2} \quad , \quad B_4 = -\frac{2(k^2+3\pi^2)}{k^2+\pi^2} \quad , \quad B_5 = -\frac{k^2+5\pi^2}{k^2+\pi^2} \quad ,$$

$$B_6 = -\frac{3(3k^4 + 2k^2\pi^2 + 15\pi^4)}{4\pi^2(k^2+\pi^2)} \quad , \quad B_7 = -\frac{25k^6 + 3k^4\pi^2 + 7k^2\pi^4 + 25\pi^6}{16\pi^4(k^2+\pi^2)} \quad , \quad B_8 = \frac{4(k^2-5\pi^2)}{k^2+\pi^2} \quad ,$$

$$B_9=\frac{6(k^4-5\pi^2)}{\pi^2(k^2+\pi^2)}\quad ,\quad B_{10}=-\frac{12(k^2+5\pi^2)}{k^2+\pi^2}\quad ,\quad B_{11}=-\frac{7k^4+12k^2\pi^2+105\pi^4}{4\pi^2(k^2+\pi^2)^2}\quad ,\quad B_{12}=\frac{12(k^2-5\pi^2)}{k^2+\pi^2}\quad ,$$

$$B_{13}=-\frac{6(k^2+5\pi^2)}{k^2+\pi^2}\quad ,\quad C_1=-\frac{4\pi^2}{k^2+\pi^2}\quad ,\quad C_2=-\frac{k^2+3\pi^2}{k^2+\pi^2}\quad ,\quad C_3=-\frac{12\pi^2}{k^2+\pi^2}\quad ,\quad C_4=-\frac{2(k^2+3\pi^2)}{k^2+\pi^2}\quad ,$$

$$C_5=-\frac{12\pi^2}{k^2+\pi^2}\quad ,\quad C_6=-\frac{2(2k^2+3\pi^2)}{k^2+\pi^2}\quad ,\quad C_7=\frac{8k^4+10k^2\pi^2-9\pi^4}{5\pi^2(k^2+\pi^2)}\quad ,\quad C_8=-\frac{20\pi^2}{k^2+\pi^2}\quad ,$$

$$C_9=-\frac{12(2k^2+21\pi^2)}{5(k^2+\pi^2)}\quad ,\quad C_{10}=-\frac{2(36k^4+k^2\pi^2+72\pi^4)}{35\pi^2(k^2+\pi^2)}\quad ,\quad C_{11}=-\frac{32\pi^2}{k^2+\pi^2}\quad ,\quad C_{12}=-\frac{72(10k^2-47\pi^2)}{35(k^2+\pi^2)}\quad ,$$

$$C_{13}=-\frac{105\pi^2}{7(k^2+\pi^2)}\quad ,\quad C_{14}=-\frac{16(47k^2+453\pi^2)}{105(k^2+\pi^2)}\quad ,\quad C_{15}=-\frac{1664\pi^2}{21(k^2+\pi^2)}\quad ,\quad C_{16}=-\frac{13504\pi^2}{231(k^2+\pi^2)}$$

Extraction and Analysis of velocity: Since the TVF is independent of time, the time derivatives on the left of equations (14) will be zero. In this case, the components of velocities are extremely sensitive to the initial guess. The analytical solutions are easily obtained for Newtonian fluid due to zero α_1, α_2 as follows:

$$w_S^N=\frac{r-1}{r}\qquad v_S^N=\pm\sqrt{\frac{4\pi^2(r-1)}{r^2(k^2+\pi^2)}}\qquad (15)$$

$$u_S^N=\pm\sqrt{\frac{4\pi^2(r-1)}{(k^2+\pi^2)}}$$

In the above equations, the index S means the steady-state and superscript N represents the Newtonian case, and it is seen that two sets of solution are obtained for the equations. If $\alpha_2 = 0$ and we consider the weakly-shear-thinning state, the equations will be simplified. These obtained equations and diagrams from weakly-shear-thinning mode should be compared to the shear-thinning and Newtonian modes. For shear-thinning mode, solving the equations above is only possible numerically, thus the appropriate initial values , which are ended to the non-trivial solutions, are found through Fortran programming software, so that we consider a desired value for r for each α_1, α_2 and guess the initial values of w_0, v_0, u_0. A subroutine, which applies Newton-Raphson algorithm, obtains w, v, u per mentioned r.

It calculates the values of w, v, u with a single value and only for a specific r, while we are seeking to find the solutions in the form of functions which give the responses per multiple values of r. Therefore, our equations should be converted into the ordinary differential equations, then we obtain $u(r), v(r), w(r)$ through another subroutine which utilizes Runge-kutta algorithm. Finally, we calculate the velocity functions by Mathematica software and compare with other cases.

Three diagrams are drawn for comparing u, v, w as follows. The comparison of these three diagrams indicates that wherever $(\alpha_2, \alpha_1 = 0)$ in the diagram related to Newtonian state, they are formed from r = 1 onwards.

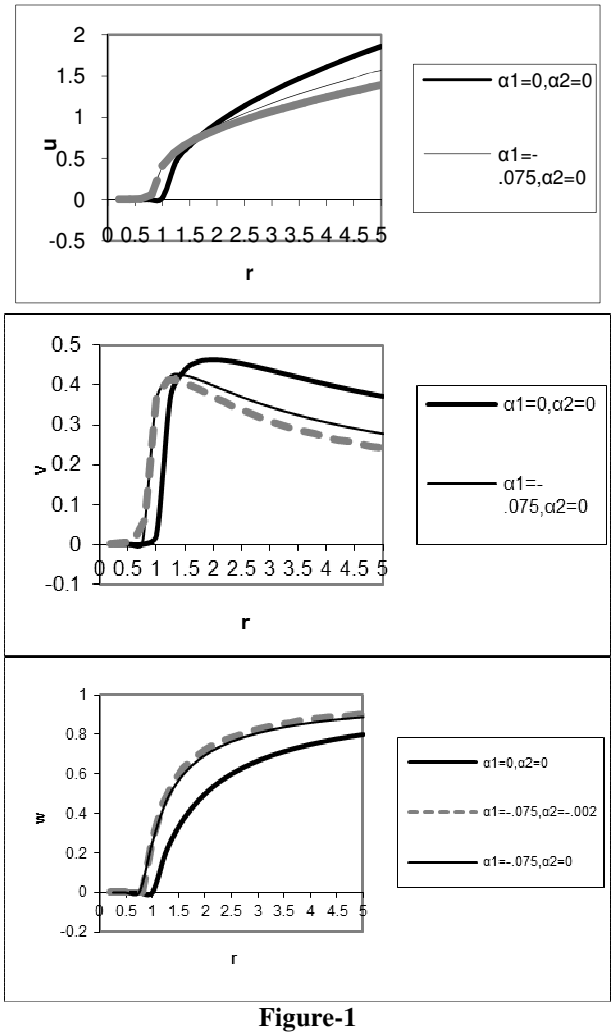

Figure-1
Obtained diagrams for u, v, w

The more the slopes of diagram are increased, the more the shear thinning is enhanced; in fact, the formation point of all diagrams indicates their critical r. We can reach this conclusion that increasing the shear-thinning property quickly makes the flow critical and u, w are enhanced by increasing Taylor number, but υ is reduced after a sharp increase. u, w are reduced by decreasing α_1, α_2, but w is increased.

Now, for obtaining the real velocities, first the time coefficients are obtained from the equations (13) and then the dimensionless velocities from equations (12) and finally the real velocities from the equations (3).

Finally, for quantitative comparison of shear-thinning effect on the velocity components, the maximum and minimum values are obtained for each velocity through the programs written in Fortran software; the results are presented in table (2).

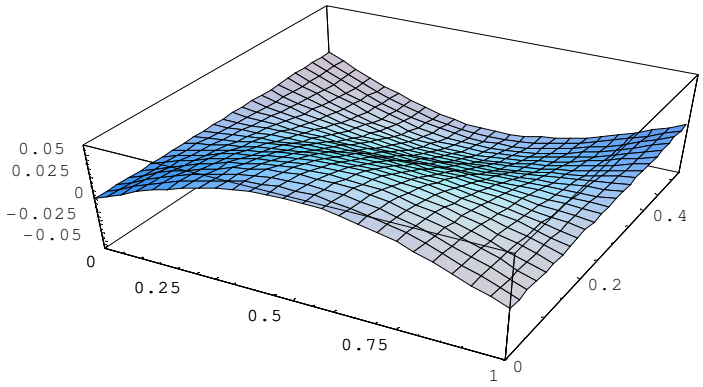

(A)

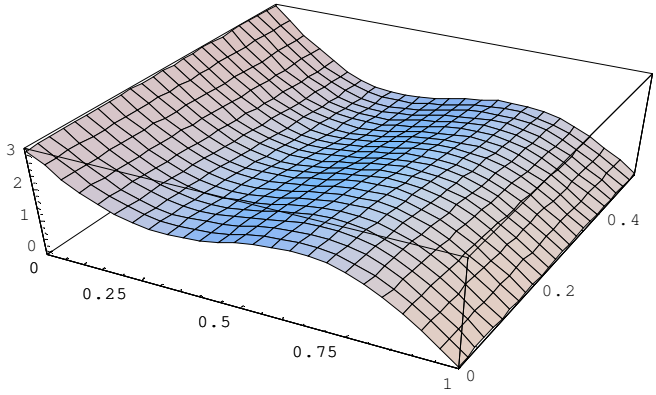

(B)

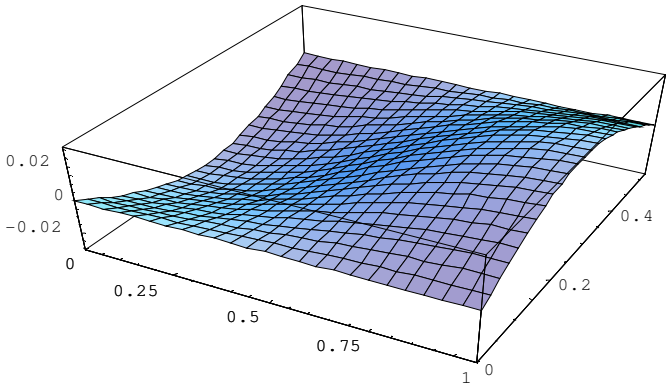

(C)

Figure-2

Spatial areas for a) U_R**, b)** U_θ**, c)** U_Z **per** $\alpha_1 = -0.075, \alpha_2 = -.002$

Table-2

Minimum and maximum values obtained for velocity components for all values of α_1, α_2

		$\alpha_1 = -0.075$, $\alpha_2 = -0.002$	$\alpha_1 = -0.05$, $\alpha_2 = -0.002$	$\alpha_1 = -0.025$, $\alpha_2 = -0.002$	$\alpha_1 = -0.01$, $\alpha_2 = -0.002$	$\alpha_1 = 0.0$, $\alpha_2 = 0.00$
U_R	Minimum	-0.055	-0.0619	-0.0648	-0.0651	-0.0663
	Maximum	0.055	0.0619	0.0648	0.0651	0.0663
U_θ	Minimum	-1.156	-1.170	-1.174	-1.175	-1.176
	Maximum	1.156	1.170	1.174	1.175	1.176
U_Z	Minimum	-0.0298	-0.0324	-0.0339	-0.0341	-0.0347
	Maximum	0.0324	0.0339	0.0341	0.0347	0.0347

Furthermore, Figure 3 shows all three states governing the components of angular velocity for a sample of α_1, α_2.

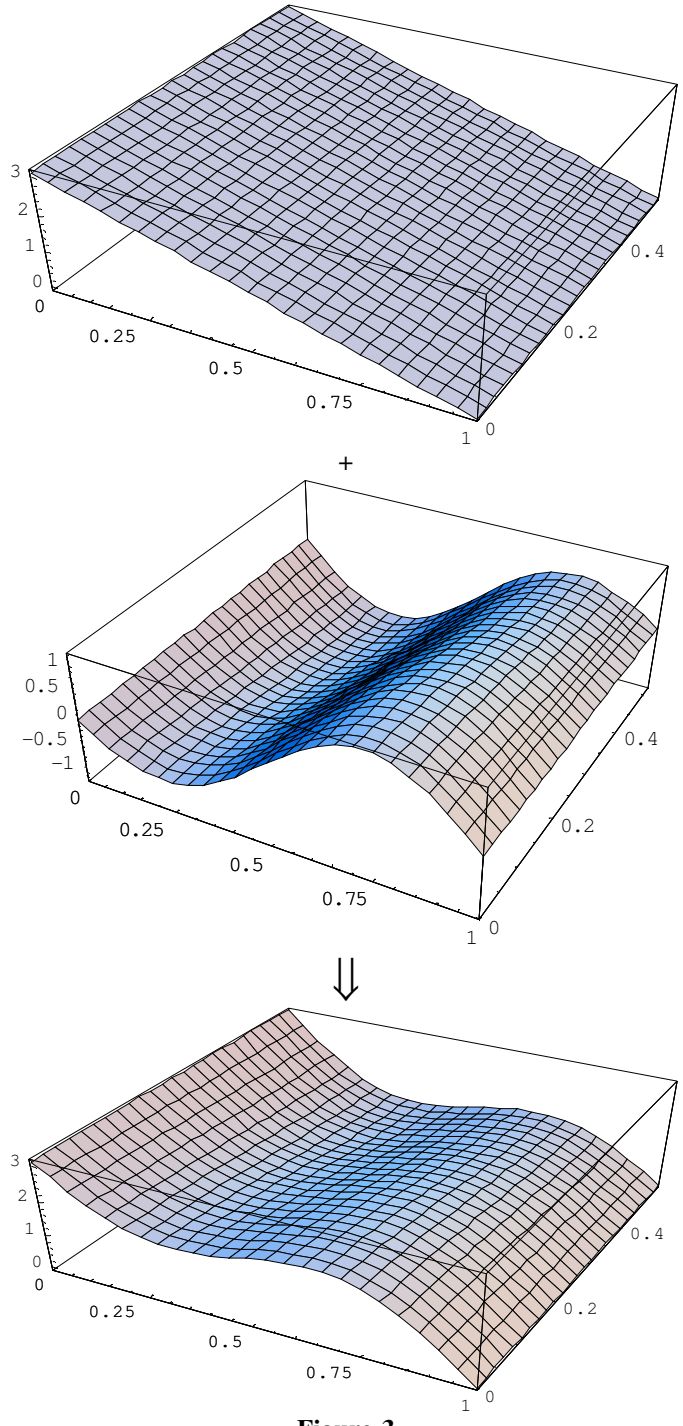

Figure-3
The real value of angular velocity obtained from the sum of components of laminar and diversion flow per

$\alpha_1 = -0.075, \alpha_2 = -.002$

The following results are obtained from the figures 2 and 3 and table 2: i. The angular velocity is significantly greater than other terms of velocities. ii. The axial and radial velocities which are not existed in the laminar flow appear due to the effects of turbulence on the TVF. It is observed that the above rates are negligible. iii. With an increase in the shear-thinning property, all components of velocity are regularly decreased. For all values of α_1, α_2, the maximum velocity is equal to π and the minimum velocity is zero m.s, which is the extreme of laminar flow. Thus, it can be found that the laminar flow is still existed and the linear flow misleads it a bit from the laminar mode. Figure 3 exactly shows this issue.

Pressure analysis and extraction: The pressure can be achieved through finding the components of velocity. According to the sixth hypothesis of second chapter, $\frac{\partial p}{\partial \theta}$ is always zero because of the axial symmetry. Moreover, $\frac{\partial p}{\partial z}$ becomes zero according to the equation for the conservation of momentum in the axial direction for the laminar flow. Therefore, the pressure will vary only along with the radius. In other words, $P^0 = P^0(x)$. According to equation (4), it can be concluded that:

$$p^0(x) = \frac{-Ta}{3}(1-x)^3 + C \qquad (16)$$

In the above equation, C is the integration constant which cannot be the function z, θ according to the arguments above and it is a constant number. Its value can be measured by measuring the pressure at a desired point. Here, its amounts is considered equal to $\frac{Ta}{3}$. [1]

Using the method used for velocity, the real pressure will be as follows:

$$p = \frac{\rho \upsilon_0^2}{d^2}\left(p_{11}(t)\cos\pi x \cos kz - \left(\frac{Ta}{3}(1-x)^3 - \frac{Ta}{3}\right)\right) \qquad (17)$$

The first term of equation above represents the diverted flow pressure and the second term represents the laminar flow pressure. Obviously, the laminar flow pressure has a greater portion of the total pressure.

The existence of Taylor number in the equation (16) indicates that the laminar flow pressure can be changed by variation in the intensity of shear-thinning; however, the pressure above will always remain constant in the laminar flow like the angular velocity because the multiplication of $\frac{\rho \upsilon_0^2 Ta}{3d^2}$ diminishes the dependence on the viscosity in measuring the real pressure.

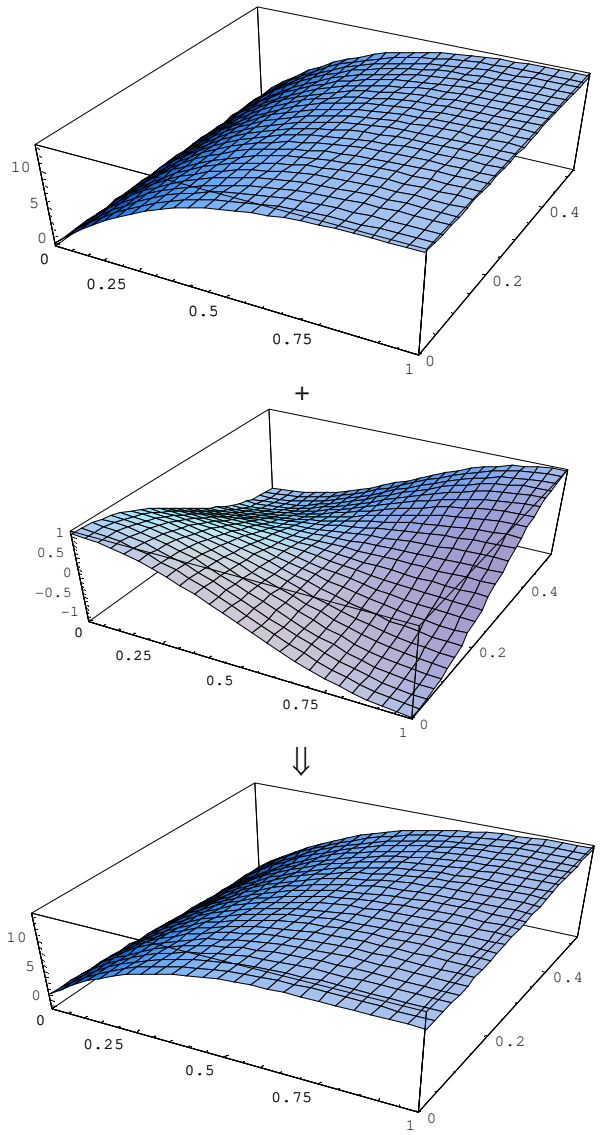

Figure-4

The real amount of pressure from the sum of laminar and diverted flows per $\alpha_1 = -.075, \alpha_2 = -.002$. The spatial areas of the fourth figure are the same as the third figure in another view

According to the selected values for the constant of integration, we have for the laminar flow:

$$P^0_{max} = 13.16 @ x = 1 \quad , \quad P^0_{min} = 0 @ x = 0 \quad (18)$$

The pressure extremes in the diverted flow include: Figure 3 and table 3 yield the following results: i. The diverted flow pressure is reduced like its velocity as the result of increasing the shear-thinning property. Here, the pressure is more reduced by reduction in x. ii. The maximum diverted flow pressure lead to the enhanced maximum total flow and its maximum reduces the maximum pressure of total flow, whereas this is not true for the velocities and the extremes of velocity in the total flow is equal to the extremes of laminar flow velocity.

Conclusion

The diverted and laminar flow parameters are analyzed through the functions, diagrams and values above and the velocity and pressure parameters in shear-thinning mode are evaluated and compared with the modes obtained from the literature and the main result of analysis above is as follows: i. In the diagrams of unreal velocities, u and w are enhanced by increasing Taylor number, but the dimensionless υ is decreased after an intense increase; u and w are decreased by enhancing the shear - thinning property, but w is increased. ii. The more the value of α_2 is reduced, the sooner the flow becomes critical. iii. The angular velocity component governs the flow at the real velocities. iv. The more the fluid progress towards the shear-thinning mode, the more the amounts of distortion at all velocities are reduced and the TVF in them decreased; in other words, it leads to the enhanced fluid capacity and resilience against the external disturbances. Thus, the fluid loses its coherence in a longer time and less influenced by the disturbance. v. The more the fluid progresses towards the shear-thinning mode, the more the amount of distortion of pressure component is reduced.

The future studies, which can be conducted to become closer to the reality in this regard, are classified into four categories: i. The study on the equation of state and investigation of other models for shear-thinning and weakly-elastic fluids for extending the range of equation above. ii. The study on the flow boundary: In this regard, the available equation of state can be utilized, thus we can analyze the fluid flow between two flat plates assuming that the walls are non-rigid. iii. This analysis can be continues assuming the oscillatory flow: The initial equations of oscillatory Taylor-Couette flow for Newtonian fluid were introduced by Kuhlmann et al.[6,7] Despite the fact that performing such this analysis is much more difficult than the non-oscillatory flow, it still seems essential[8-10]. iv. Analyzing the flow based on the not centralized cylinders[11,12].

Table-3

The minimum and maximum values obtained for the pressure component in terms of all values of α_1, α_2

		$\alpha_1 = -0.075$, $\alpha_2 = -0.002$	$\alpha_1 = -0.05$, $\alpha_2 = -0.002$	$\alpha_1 = -0.025$, $\alpha_2 = -0.002$	$\alpha_1 = -0.01$, $\alpha_2 = -0.002$	$\alpha_1 = 0.0$, $\alpha_2 = 0.00$
P(pa)	Minimum	-1.081	-1.082	-1.083	-1.243	-1.33
	Maximum	1.081	1.082	1.083	1.243	1.33

References

1. Ashrafi N. and Khayat R.E., Shear-thinning Induced Chaos in Taylor-Couette Flow, *Physical Review*, **61(2),** 1455-146 **(2000)**

2. Kuhlmann H., Model for Taylor-Couette Flow, *Physical Review*, **32(3),** 1703-1707 **(1985)**

3. Roland L., Panton, Incompressible flow, A wiley Interscience publication, chap 6 and 747-751 **(1996)**

4. Hlavacek M., A central film thickness Formula for elastohydrodynamic lubrication of Cylinders with soft incompressible coatings and a Non- Newtonian piecewise power-low lubrication Steady rolling motion, wear, **205**, 20-27 **(1997)**

5. Kuhlmann H., Roth D., and Lucke M., Taylor Vortex Flow under Harmonic Modulation of the Driving Force, *Physical Review*, **39(2),** 745-762 **(1989)**

6. Bird R.B., Armstrong R.C. and Hassager O., Dynamics of Polymeric Liquids, John Wiley & Sons, Chap. 4 **(1987)**

7. Chossat P. and Looss G., The Couette-Taylor Problem," Springer-Verlag, Chap.'s. 1,2, 3 **(1994)**

8. Mohan Lal and Gangotri K.M,A Comparative study on the Performance of Photogalvanic cells with mixed Surfactant for Solar Energy conversion and storage: D-Xylose-Methylene Blue systems, *Res. J. Recent Sci.,* **2(12),** 19-27 **(2013)**

9. Chikwe T.N., Osuji L.C., Ogali R.E. and Okoye I.P. Effects of Petroleum Condensate/Diesel Mixture on Diesel Engines, *Res. J. Recent Sci.,* **2(1),** 1-8 **(2013)**

10. Mojtaba Khalili, Azim Akbarzadeh, Mohsen Chiani and Sepideh Torabi, The effect of Nanoliposomal and PE Gylated Nanoliposomal Forms of 6-Gingerol on Breast Cancer Cells, *Res. J. Recent Sci.,* **2(5),** 29-33 **(2013)**

11. Dileep E., Nebish M. and Loganathan V. Aerodynamic Performance Optimization of Smart Wing Using SMA Actuator, *Res. J. Recent Sci*, **2(6),** 17-22 **(2013)**

12. Mussarat Yasmin, Muhammad Sharif, Sajjad Mohsin, Use of Low Level Features for Content Based Image Retrieval: Survey, *Res. J. Recent Sci.,* **2(11),** 65-75 **(2013)**